Journal of Electroceramics, 12, 53–68, 2004
© 2004 Kluwer Academic Publishers. Manufactured in The Netherlands.

Submicrometer-Scale Patterning of Ceramic Thin Films

C.R. MARTIN & I.A. AKSAY

Department of Chemical Engineering, Princeton University, Princeton, NJ 08544-5263, USA

Abstract. The patterning of ceramic thin films is of great interest for use in MEMS and other applications. However, the complex chemistries of certain materials make the use of traditional photolithography techniques prohibitive. In this paper, a number of low-cost, high throughput techniques for the patterning of ceramic thin films derived from chemical solution precursors, such as sol-gels and ceramic slurries, are presented. A particular emphasis is placed on methods that are derived from soft lithographic methods using elastomer molds. Two categories of techniques are discussed: first, the focus is on methods that rely on the principles of confinement within the physical features of the mold to define the pattern on the substrate surface. Then, subtractive patterning techniques that rely on transferring a pattern to a spin-cast, large-area continuous thin film are described. While most techniques have been demonstrated with fidelities on the order of 100 nm, their inability to precisely register and align the patterns as part of a hierarchical fabrication scheme have thus far hindered their commercial implementation.

Keywords: patterning, ceramic, thin films

1. Introduction

The advent of the electronic age has been the primary driving force for the development of thin film technologies for semiconductor applications, including techniques for the definition of submicrometer-scale patterns [1]. A typical microfabrication process utilizes photolithography [2] with photo-curable polymers to define patterns that are transferred to thin films of metal and semiconductor materials comprising the integrated circuit (IC) by wet or dry chemical etching. Many of these techniques have been transferred to materials with specialized properties for new engineering applications, such as microelectromechanical systems (MEMS) capable of sensing [3], actuation, information processing [4], optical waveguides, surface acoustic wave devices, and holographic memories [5]. For example, Ozawa and Yao [6] demonstrated the use of a photolithography lift-off process to pattern TiO_2 thin films with line widths as small as 1 μm. Similarly, Nashimoto et al. [7] fabricated 5 μm wide $(Pb,La)(Zr,Ti)O_3$ waveguides by using wet chemical etching with HCl prior to heat treatment.

Unfortunately, the utility of applying conventional photolithography techniques to ceramics in general can be limited by the chemistry of the material. For instance, the integration of ferroelectric materials, such as lead zirconate titanate ($PbZr_xTi_{1-x}O_3$, PZT), in electronic devices such as capacitors, transducers, pyroelectric devices, thermosistors, and dielectrics is a field attracting considerable attention [8]. However, traditional subtractive patterning steps are of limited utility to materials such as PZT because many of the solvents and acids used to etch silicon, such as HF, are not compatible with PZT. Instead, Reactive Ion Etching (RIE) must be used, which is very costly due to the requirements of specialized equipment with controlled environments and waste control systems to minimize lead contamination [9].

During the past decade, a number of alternative techniques to traditional photolithography for patterning a variety of materials have been developed [10]. The motivation for this work stems from four reasons: (1) lower cost and ease of use than the capital intensive equipment required for photolithography, (2) the ability to apply patterning techniques to new materials, (3) the potential to pattern large areas simultaneously, and (4) the ability to pattern on nanometer length scales that are not yet commercially produced by lithography. This paper focuses on techniques developed to address the first three motivations. Specifically,

we highlight the development of patterning methodologies on the submicrometer length scale that can be applied to a wide range of ceramic thin film materials. Patterning on smaller nanometer length scales is not our specific goal due to the propensity for many ferroelectric materials to lose particular properties that make them of interest for MEMS and other applications in the first place. For example, lead titanate loses its piezoelectric properties in grains smaller than 20 nm [11].

Consistent with the objective of low cost processes, the discussion will be limited to methods that do not require large expenditures of capital equipment beyond what would be found in a basic microfabrication laboratory equipped for photolithography. As a result, our focus will be on materials that can be deposited and patterned using liquid precursors, such as sol-gels [12, 13] or colloidal suspensions. We will also further restrict our discussion by neglecting serial patterning techniques, such as ink-jet printing [14–16], as these are not viable techniques for scaling production to the commercial applications that require the ability to pattern large areas simultaneously.

The paper is divided into two sections. First, patterning methods that are based on the principle of physical confinement of the precursor solution are discussed. The second section of the paper highlights a pair of patterning techniques that are based on the spin-casting of a large area thin film and then producing the final pattern by subtractive means. The discussion of each technique includes examples of ceramic materials that have been patterned by the method with emphasis on the length scale of the resolution limit.

Many of the techniques illustrated in this paper are derivatives of the methods developed by the Whitesides group at Harvard University [10], as soft lithography is more convenient and lower in cost than the traditional subtractive methods. This is a very active area of research in its application to ceramic thin films, as the majority of the available literature has been published within in the past five years.

Soft lithography requires the use of an elastomeric mold patterned with relief structures on its surface. First, a lithographic master with complex three dimensional patterns is fabricated using conventional photolithography, micromachining, or electron beam writing techniques. Using cast molding, a negative of the patterns of the master is produced in the elastomeric stamp, as shown in the center panel of Fig. 1 [10].

The most common elastomeric material used in soft lithography is poly(dimethylsiloxane) (PDMS), though other materials may be used. The low surface energy of PDMS ($\gamma_{\text{PDMS-air}} = 0.0216$ N/m, compared to $\gamma_{\text{Si/SiO}_2\text{-air}} \sim 0.072$ N/m) allows it to be easily released from the master after curing, as well as from the substrate and the dried material after patterning. PDMS is not hydroscopic and does not swell when in contact with water. It has not been found to react with or swell due to contact with many of the compounds and solvents present in chemical precursor solutions. The PDMS is thermally stable to 186°C, allowing for the use of moderate heat to quickly cure the mold. The material is isotropic and homogeneous, allowing it to be used to pattern over large areas in future applications. Further, PDMS is permeable to gaseous molecules, a critical property for allowing the patterned chemical solution or colloidal suspension to dry within the confines of the mold [10].

Conveniently, the materials for casting PDMS molds are available commercially; most research groups use Sylgard$^{\text{TM}}$ 184, a two-part kit manufactured by Dow Corning (Midland, MI). To prepare the PDMS for casting, a 10:1 ratio of the liquid silicon rubber base, containing primarily vinyl-terminated PDMS, is mixed with a curing agent that promotes hydrosilylation reactions to cross-link the network and produce a solid elastomer [10]. Feature sizes as small as 30 nm have been patterned on a PDMS mold [17].

With the exception of the preparation of the lithographic master, soft lithography does not require the use of a clean room or expensive microfabrication equipment. Once a lithographic master is available, the master can be reused multiple times for templating PDMS molds. Thus, the various soft lithography techniques are very much available in terms of time and cost. In addition, the use of elastomers for the mold in soft lithography adds a degree of flexibility not found in a mask used in photolithography, as the molds can be deformed by mechanical compression, tension, or strain to conform to curved substrates or manipulate the desired patterned features sizes [10].

There are potential disadvantages of soft lithography that need to be overcome before it is readily implemented in commercial practice. First, PDMS shrinks by approximately 1% during curing and can be swelled by nonpolar organic solvents such as toluene and hexane. The softness of the elastomeric material can cause

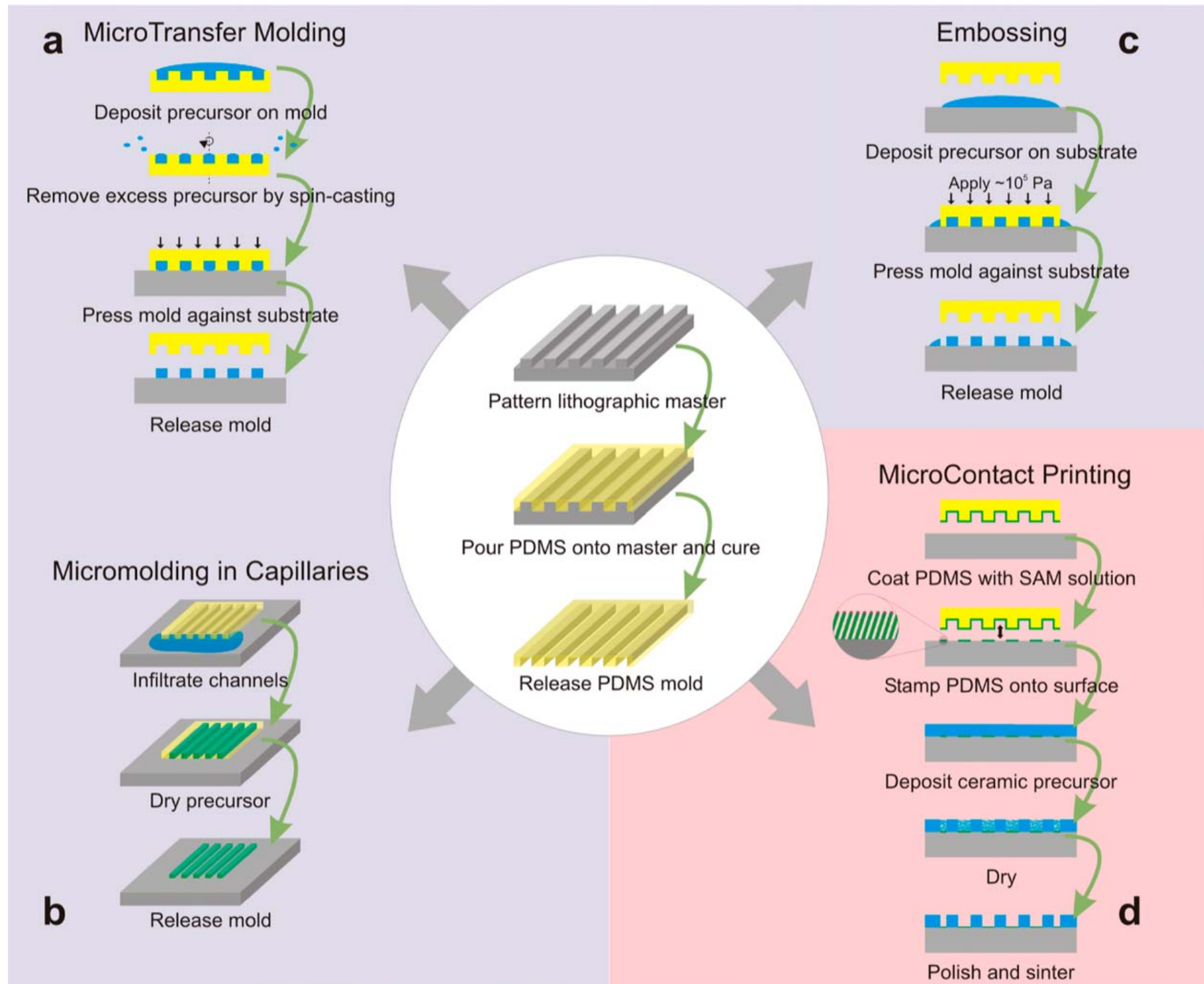

Fig. 1. Schematic illustration of PDMS mold preparation and soft lithography techniques used to pattern ceramic materials. (a) MicroTransfer Molding, (b) Micromolding in Capillaries, and (c) Embossing are confinement-based techniques while (d) MicroContact Printing is based on the principles of surface modification.

features to deform or distort, such as sagging or buckling channels, if insufficient attention is paid to the aspect ratio of the microstructures [10]. This second issue can be partially mitigated by the use of composite stamps, particularly for producing free-standing features smaller than 100 nm [18]. But most critically, it is difficult to design a scheme to register the PDMS molds with the substrate during the fabrication of multiple layered structures [19]. It is this point in particular that led to the development of a class of hybrid photolithography/soft lithography casting schemes, such as the MicroChannel Molding (μCM) technique developed by the authors [20].

2. Confinement-Based Techniques

The philosophy shared by the following confinement-based techniques is that the pattern is imparted to the thin film by using physical boundaries to define where the chemical precursor solution or colloidal suspension dries and rigidifies. Each of these methods is an additive patterning technique, whereby the material is deposited to the substrate only where desired in the final pattern. In general, this is advantageous to subtractive patterning techniques such as etching, as the methods tend to require fewer processing steps. In industrial practice, these methods may also

result in less waste, reducing disposal and raw material costs.

The first two methods, MicroTransfer Molding (μTM) [21] and Micromolding in Capillaries (MIMIC) [22–24], are each soft lithography techniques that rely on the filling and duplication of the three dimensional topography of the mold followed by the release of the elastomer to transfer the pattern solely to the substrate. The third technique, embossing, relies on the displacement of material by the protruding features of the mold to effect the pattern to the thin film. Embossing can use either molds fabricated from hard materials, as well as elastomers. The resolution of the patterned material is determined by interfacial energies that determine the wetting of the precursor solution with the solid surfaces and the ability of the mold to detach from the patterned material after drying. Kinetic factors such as filling of the mold and gelation time also play a role in determining the fidelity of the final pattern [10]. Each of these techniques produces a negative replica of the pattern in the mold, or a positive replica of the original lithographic master. These techniques can be used to produce features that have variable feature heights unlike traditional photolithography. However, they also suffer some of the same disadvantages and limitations associated with soft lithography, such as the limited ability to register the patterns in hierarchical structures.

A fourth class of techniques based on the principles of casting is presented in this paper. The problem of pattern registry is overcome by placing the relief pattern for confinement on the substrate to be patterned instead of the disposable mold. Well-established photolithography techniques, or even other soft lithography methods, can be used to pattern the relief features used to cast the thin film, but at the expense of additional processing steps required to remove the relief features at the end.

2.1. MicroTransfer Molding

In μTM [21], a prepolymer or chemical precursor solution is deposited into the recessed regions of the patterned side of the stamp, most commonly by spin-casting. The stamp is then brought into contact with the substrate. The lower interfacial energy of the PDMS relative to the substrate allows for the patterned material to remain on the surface as the stamp is peeled away [10]. The material is then ready for heat treatment. The μTM process is illustrated schematically in Fig. 1(a) [25]. μTM is a very rapid patterning method capable of patterning very large areas simultaneously.

An analysis of the process indicates that for proper pattern transfer poor adhesion of the "ink" with the stamp is required with a wetting angle of greater than 90°. This allows for the solution to pull away from the walls of the recessed channels when the ink dries during the spin-coating step. Any remaining bonds between the ink and the PDMS must be broken during the stamping step from the imposed mechanical stress [26, 27]. These constraints require the careful tuning of solution precursor properties to the interfacial energy of the elastomeric stamp and surface to obtain high quality films with complete pattern transfer to the substrate.

The Whitesides group [21] used commercial spin-on glass and ZrO_2 precursors to demonstrate the utility of μTM to pattern ceramic materials. Meanwhile, Moran and Lange [26] patterned monoclinic zirconia lines orientated epitaxially from a zirconyl 2-ethylhexanoate precursor solution with 500 nm lines widths, as shown in the scanning electron microscope (SEM) image in Fig. 2. Kim et al. [25] demonstrated the use of μTM with perovskite metal oxide structures, by patterning 50 μm wide $SrBi_2Ta_2O_9$ (SBT) lines on a (001) $SrTiO_3$ substrate. Using ceramic powders of alumina, boehmite [28], zirconia, cerium gadolinium oxide, and tin oxide [27], the Gauckler group used PDMS molds to cast suspensions and sinter the dried patterns to produce line widths as small as 3 μm. However, instead of releasing the patterned film against a substrate, they released the ceramic structures as free-standing microscale objects. Similarly, Su et al. [29] fabricated free-standing

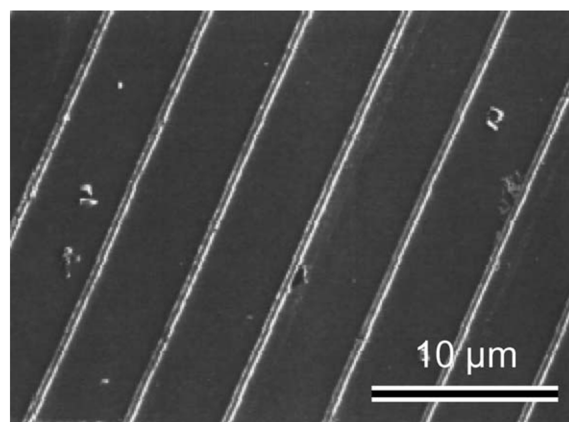

Fig. 2. 500 nm wide ZrO_2 lines patterned by μTM [26].

alumina microgears using centrifugal casting of alumina suspensions into PDMS molds.

No one has yet demonstrated the use of μTM in the fabrication of a hierarchical structure. In addition to the pattern alignment issues associated with soft lithography, μTM adds the complexity of trying to align the pattern with the presence of a drying, time-sensitive material on the surface of the mold. This operational handicap may prevent the ability to produce well-controlled features with the degree of reproducibility required for commercial applications.

2.2. *Micromolding in Capillaries*

MIMIC has received perhaps the most attention of the primary soft lithography molding techniques for use in patterning ceramic materials [22–24]. It is a single step process that has been used successfully to pattern a wide variety of materials, including photo- and thermally-curable prepolymers, ceramics, metals (in conjunction with electroless deposition), colloidal particles, and biologically functional macromolecules [10, 24]. The PDMS mold is placed with the patterned surface down on the substrate to form a network of microcapillary channels. The elastomer must be cut beforehand to expose the entrance of the channels for the liquid to enter. A pool of solution is placed at the entrance of the channels. Capillary action spontaneously draws the liquid into the channels to fill them. The permeability of the PDMS to water and organic vapors permits the use of MIMIC in applications with sol-gels and colloidal suspensions that need to dry and cure [10]. After gelation and drying, the mold is released from the patterned substrate. This procedure is illustrated in Fig. 1(b).

This is a process driven by the thermodynamics of minimizing the total interfacial energy of the system as the solid-vapor and solid-liquid interfacial areas change. To continue to fill the channels, the capillary pressure at the meniscus must be greater than the hydrodynamic pressure drop along the already-filled distance of the channel. As a result, the rate of capillary filling is inversely proportional to the distance that has already been filled, as expressed by

$$\frac{dz}{dt} = \frac{R\gamma_{LV}\cos\theta}{4\eta z} = \frac{R(\gamma_{SV} - \gamma_{SL})}{4\eta z}, \qquad (6)$$

where R is the hydraulic radius of the channel, z is the penetration distance of the fluid in the channel, η is the viscosity of the solution, θ is the contact angle of the liquid on the PDMS surface, and γ_{SV}, γ_{SL}, and γ_{LV} correspond to the PDMS-vapor, PDMS-liquid, and liquid-vapor interfacial free energies, respectively [22, 30]. Typical capillary filling distances are on the order of 1 cm [10]. Because capillary pressures for channels of radius from 1 to 10 μm are on the same order as atmospheric pressure, the filling distances can be enhanced by the use of a vacuum pump at one end of the channels [31]. The rate of capillary filling is proportional to the hydraulic radius of the channel, indicating the higher capillary pressures of smaller capillaries is more than offset by the increased resistance from the channel surfaces. Further, it is important to control the viscosity of the filling fluid because the rate is inversely proportional to the viscosity of the precursor solution. The sol-gels that we use have viscosities on the order of 0.01 Pa·s.

While the size and shape of the features to be patterned are very flexible, it is also important to note that the method requires a network of connected channels. The method cannot be used to pattern an array of isolated dots or features. The procedure requires the removal of excess dried precursor solution that gelled outside the confines of the mold, in this case from the liquid from the original pool that did not infiltrate the channels. Unlike μTM, patterning is not a very rapid process as the filling of the capillary channels as it can take over a day when using a sol-gel.

The most serious limitation of the process when applying the process to colloidal suspensions and sol-gels is that the solution being patterned rarely fills the entire channel in the vertical direction after the volumetric shrinkage that results from the drying of the solvent. In the case of the PZT synthesized by a chelation-modified sol-gel chemistry [32, 33], the final sintered material comprises only 18% of the original volume [34]. This can result in deviations of the topography from the shape of the original mold, as demonstrated by the atomic force microscopy (AFM) scans of sintered PZT pattern shown in Fig. 3(b). These topographical defects are most pronounced when using molds with features such as corners whose radius of curvature is much smaller than the width of the mold. The presence of sharp corners causes accelerated drying and slower dewetting which combine to produce "double-peak" topographies in the patterned thin films [34].

The application of MIMIC to ceramics was first demonstrated by the Whitesides group using a SiO_2 sol-gel precursor [24]. Xia et al. have applied the method

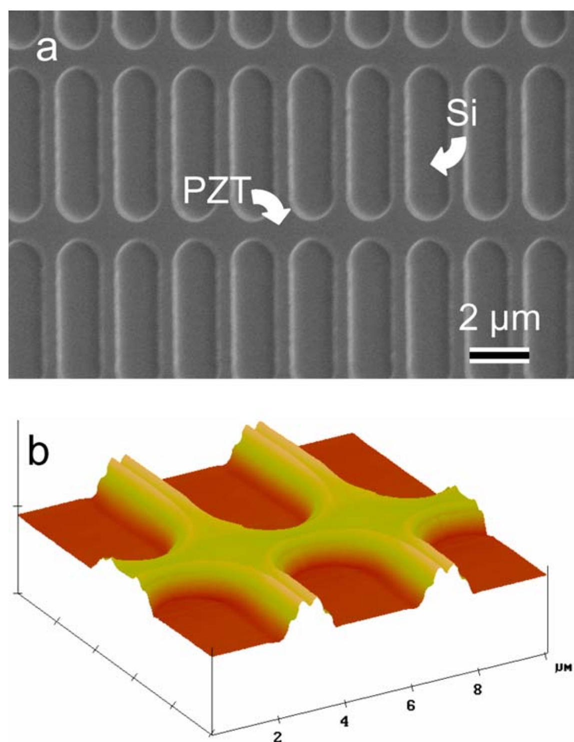

Fig. 3. (a) SEM image of a grid pattern of PZT lines patterned from 1 μm wide channels. (b) AFM topography scan of 2 μm wide PZT lines that shows the "double-peak" topographical distortion that forms during drying and sintering.

to the patterning of structural oxide ceramics such as ZrO_2 [10, 35] and tin dioxide (SnO_2) [35]. The first ferroelectric ceramics patterned by MIMIC used PZT derived by the chelation synthesis route by researchers at the University of Washington [36] and the Aksay group [33, 34]. A grid of 1 μm wide PZT lines patterned on a silicon wafer is shown in Fig. 3. The University of Washington group also reported the patterning of piezoelectric strontium niobate ($Sr_2Nb_2O_7$) [36]. The Aksay group also augmented the capillary forces with electric fields to infiltrate the microcapillary channels with mesoscopic silica system with hexagonally-arranged cylindrical micelles; conveniently, this electric field was found to have the effect of aligning the nanometer-scale tubules in an axial alignment with the applied field [37, 38]. Yang et al. [39] used MIMIC to pattern a suspension of 200 nm polystyrene microspheres. The colloids arranged themselves in a FCC lattice within the confines of the channels. After drying with the mold in place, a precursor mesoscopic silica precursor solution was infiltrated into the channels. The polystyrene template was removed by pyrolysis after the sol-gel dried. The result is the simultaneous patterning of cubic mesoporous silica on the three discrete length scales of 10 nm, 100 nm, and 1 μm.

Most recently, researchers at the Chinese Academy of Sciences used MIMIC with sol-gel chemistry to pattern phosphor thin films [40] and silica films doped with organic dyes [41]. Heule and Gauckler [42] patterned SnO_2 from a slurry for use in a gas sensor, one of the first demonstrations of incorporating soft lithography with a ceramic material for use in functional device. Microscopy images and a schematic diagram of their device are shown in Fig. 4. MIMIC has been used to pattern defect-free regions of line widths as small as 400 to 500 nm with a surface coverage of 1 cm^2 [33, 35]. The viscosity of most chemical solution precursors limits the ability to fill capillary channels smaller than this length scale over appreciable distances, placing a lower bound on the possible resolution that can be achieved by MIMIC.

2.3. *Embossing*

Embossing is a very active area of research, particularly among those interested in fabricating complicated three-dimensional structures for MEMS [43]. A continuous film layer is deposited onto the substrate and then patterned by forceful application of a mold. It is similar in principle to injection molding except pressure is applied directly to the mold, not the fluid. It has gained tremendous use for patterning polymers, due to the ability to control the rheological properties using temperature. This feature has permitted the ability to pattern polymer thin films on the nanometer length scale, a process commonly referred to as nanoimprinting [44, 45].

The use of embossing to patterning ceramic films derived from sol-gels or colloidal slurries adds the complexity of not being able precisely control the fluid rheological and wetting properties during the process. Care must be used to select the proper system of substrate, mold, and solution to produce crack-free patterns with the desired fidelity.

When using a liquid precursor such as a sol-gel, PDMS stamps are a common choice for the mold. A film of the precursor solution is deposited on the substrate. The PDMS mold is pressed against the substrate with a pressure of approximately 10^5 Pa [39, 46]. For a

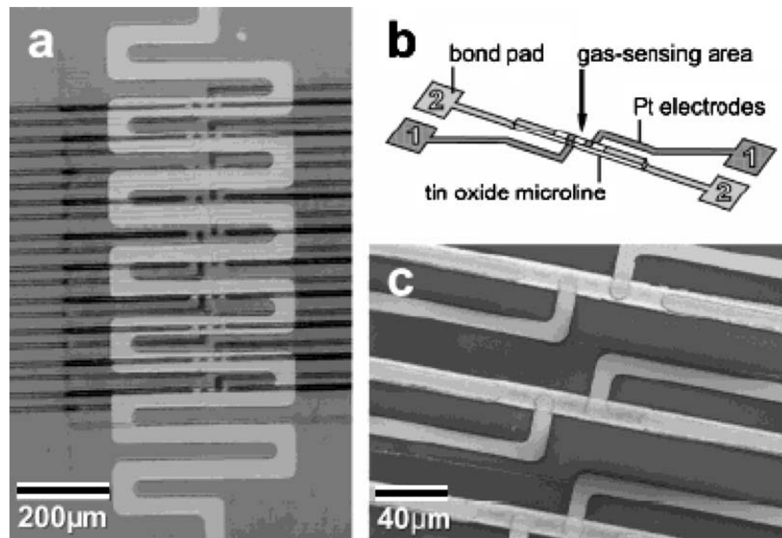

Fig. 4. Gas sensor fabricated by Heule and Gauckler [42] using micromolding in capillaries. (a) Top view as viewed through an optical microscope in which the dark horizontal lines are the patterned tin oxide features. (b) Schematic of the device. (c) SEM image of the device showing the platinum contact lines contacting the tin oxide features.

high quality pattern to develop, it is imperative for the solution to dewet from the regions where no solution is desired to allow the raised features of the mold to contact the substrate. The dewetting is driven by the applied pressure and difference in surface tensions of the solution and elastomer [46]. Frequently, the addition of a polar solvent is used to enhance the dewetting of the film from the substrate, a variation of the technique that is called Solvent-Assisted Micromolding (SAMIM) [10, 46]. When using PDMS stamps, it is important not to use too much force as this could cause the features of the stamp to buckle or deform. For the same reason, the features on the elastomer should be limited to an aspect ratio between 0.5 and 2 [47].

When the stamp in contact with the substrate, the solution is allowed to gel and dry. Once cured, the mold can be released from the substrate, and the patterned material is ready for heat treatment for further drying and sintering. The process is illustrated schematically in Fig. 1(c) [46]. As for μTM and MIMIC, the production of a high resolution pattern in the thin film requires the selection of a stamp that has significantly lower adhesion energy with the material than the material has with the substrate. One limitation of this process is that some dried material may remain on the substrate around the edges of stamp that may need to be removed.

Liquid embossing with PDMS molds was first used by the Whitesides group [46] to selectively deposit silica glass doped with boron oxide, titanium oxide, or aluminum oxide from sol-gel solutions on silicon wafers. These patterned waveguides are shown in the SEM images in Fig. 5. Yang et al. [39] patterned mesostructured $SiO_2, Nb_2O_5, TiO_2, ZrO_2, WO_3$, $AlSiO_{3.5}$, and $SiTiO_4$ with features on the 100 nm length scale. Bulthaup et al. [43] demonstrated the use of liquid embossing to fabricate inorganic hierarchical structures such as transistors, photodetectors, and resistors with features as small as 120 nm. Commercial spin-on glass, semiconducting CdSe nanocrystals, and Au nanocrystals dispersed in α-terpineol were each embossed to fabricate a thin film transistor (TFT) with a field effect mobility of 0.1 $cm^2 \cdot V^{-1} \cdot s^{-1}$ and an on/off ratio of 10^3. These results compare favorably with all-printed inorganic TFTs.

Due to the difficulty in achieving complete dewetting of the fluid where the relief structures press into the thin film, embossing has found much greater use in applications where complete removal of the fluid is not required. For example, Schueller et al. [48] fabricated a two-dimensional photonic crystal structure for lasing applications by a curing a 2 μm thick film of organically-modified silicate compressed between the substrate and a PDMS mold with 50 nm

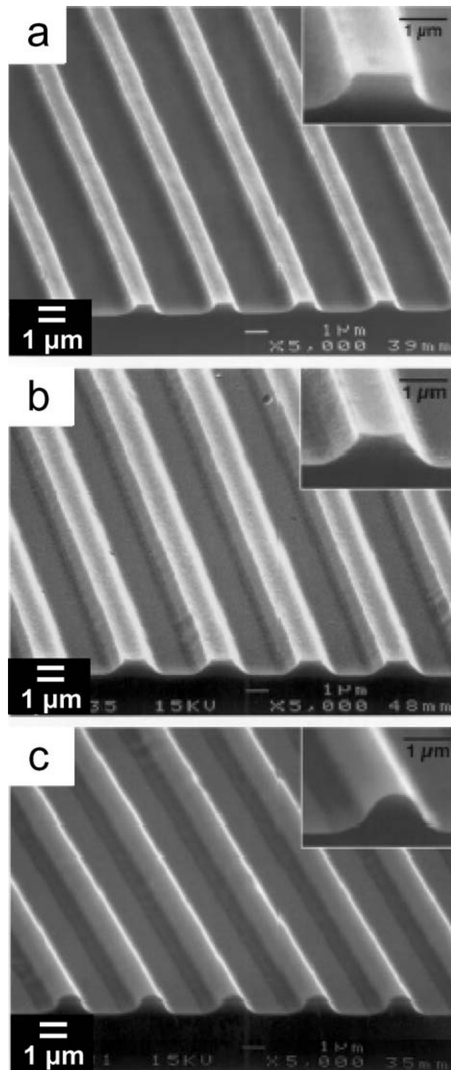

Fig. 5. Waveguides patterned by embossing on a silicon substrate by Marzolin et al. [46]: (a) aluminosilicate (Al/Si = 0.09); borosilicate (B/Si = 0.1) annealed for 10 min at 800°C (b) and 900°C (c).

high circular protrusions arranged in a hexagonal arrangement. The smallest lateral dimension of the features was approximately 150 nm and the measured optical threshold was consistent with resonators fabricated by conventional photolithography techniques in thermally-grown silicon oxide. Matsuda et al. [49] patterned grooves of pitch 1.6 μm and depth 86 nm in gel films of $CH_3SiO_{3/2}$-SiO_2 for optical data storage applications.

When using ceramic slurries, harder masks that are less prone to deformation are favored over elastomers due to the requirement of increased pressures. Petronis et al. [50] used SiO_2 masks with a hexagonally-arranged pattern of 200 μm circles spaced 100 μm to produce titania green bodies by both embossing and injection-molding. After heat treatment, a ceramic scaffold was produced for hepatocyte cell cultures. Su et al. [29, 51, 52] embossed the surface of PZT viscous polymer processed (VPP) tapes with 10 to 150 μm features and 3 to 10 aspect ratios using polymethyl methacrylate (PMMA) molds. The embossing required pressures of 10^7 Pa and the green body was removed from the mold by chemical dissolution of the PMMA or laser ablation.

While embossing may be a fast and practical method for producing patterned features, the use of significant pressures to impart the pattern may prohibit the use of embossing in certain applications with brittle substrates. The process has not yet been demonstrated in a functional device requiring hierarchical processing steps. Embossing may be limited to the steps at the beginning of the procedure when the substrate surface is relatively planar; potentially, the applied pressures used in embossing may distort or alter any features that may have been previously fabricated on a surface.

2.4. *Casting*

Despite the large interest in soft lithography techniques, it has not yet met with wide commercial success. The primary reason is that registry of the patterns produced with soft lithography to fabricate hierarchical structures remains problematic. Some progress has been made by attaching the PDMS mold to a glass slide and aligning the patterns with a light optical microscope [19]. New techniques that combine the principles of soft lithography with traditional photolithography equipment and materials may hold the greatest promise for commercial use. In the following casting techniques, the substrate surface is patterned with the relief features that form the mold for patterning the ceramic precursor solutions.

Schönholzer et al. [53] used a casting technique called photoresist molding to pattern alumina and zirconia thin films derived from colloidal suspensions. Nearly defect-free regions of 1 cm^2 with features with line widths of five microns and aspect ratios less than one have been produced. Traditional photolithography is used to pattern a polymer photoresist on a flat substrate. The combination of the substrate and patterned photoresist forms the “mold.” A ceramic suspension

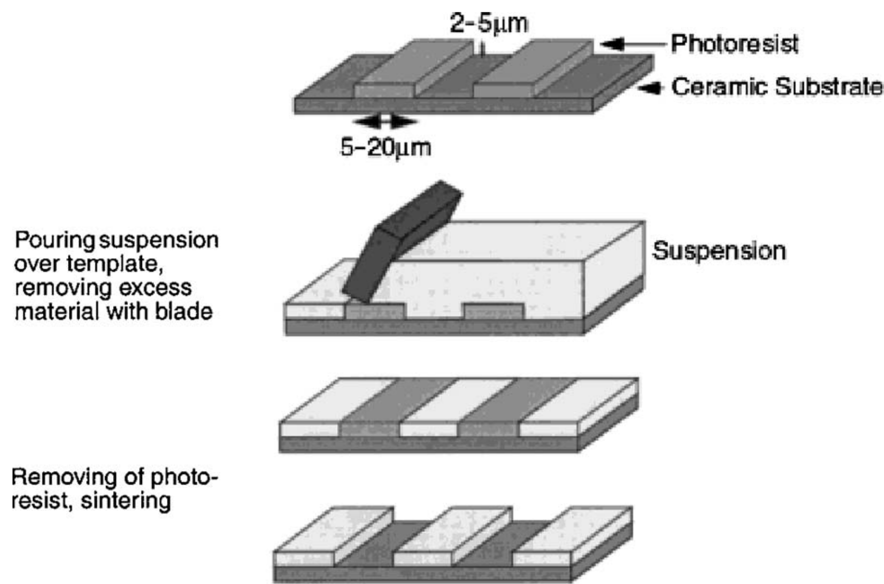

Fig. 6. Schematic diagram of photoresist molding developed by Schönholzer et al. [53].

with high solids loading is poured on top of the mold and a polymer blade is swept across the surface to remove the excess liquid. The process is illustrated in Fig. 6. The thin ceramic layer dries nearly instaneously and leaves behind residual supernatant particles on the photoresist regions. These particles can be removed by contacting the filled mold with an adhesive tape, gently pressing into the sample, and then peeling off the tape. The photoresist is removed by dipping the substrate in a beaker of acetone prior to the heat treatment of the patterned ceramic thin film.

This technique has not yet been adapted for use with materials derived from sol-gels or other chemical solution precursors. One reason may be that many sol-gels contain organic solvents that dissolve commercial photoresist. To mitigate this problem, the photoresist mold would have to be replaced with a different polymer. This polymer could potentially be patterned by any of the soft lithography techniques introduced earlier to eliminate the reliance on using photolithography for definition of the pattern. Further, no studies of the patterned material have been performed to evaluate whether the shear stresses imposed during wiping step produce any anisotropic properties in the resulting material.

Using the same idea of preparing a pattern for casting on the substrate surface, we developed a hybrid approach called MicroChannel Molding (μCM) that combines photolithography with MIMIC [20]. The motivation stems from being able to leverage the key advantage of MIMIC, the ability to pattern on submicrometer length scales, while solving the problems of pattern registry and topographical deformation. In μCM, a continuous thin film of material is deposited on the substrate surface and patterned using traditional photolithography. A flat, unpatterned PDMS membrane is placed across the top of the sample to form the network of capillary channels for infiltration. The substrate surface forms the bottom, the patterned thin film forms the sidewalls, and the PDMS membrane forms the top of the channel. The pool of liquid precursor is placed at the entrance to channels, allowing capillary forces to draw the fluid into the network. As in MIMIC, this approach is limited to patterns with interconnected capillary channels; isolated features can not be patterned.

The topographical profile of the resulting patterns is much more representative of the shape of the original channels. This is because the permeable PDMS membrane is located only at the top surface of the channel, producing a one dimensional evaporation profile. Without the amplified drying rates at the corners of the noncircular capillary channels, the drying material does not lock in the shape of the corner significantly earlier than the rest of the thin film, eliminating the formation of the double-peaked topographical

profile that develop in thin films patterned by MIMIC.

One disadvantage of μCM is that thin film used for "casting" or molding must be compatible with the sol-gel or suspension to be patterned. For example, when patterning our PZT thin films, the isopropanol in the sol-gel partially dissolves most commercial photoresists. Further, the dried PZT gel is removed when using acetone to remove the photoresist so it must be heat treated to convert it to desired crystal structure first. But sintering takes place at 600°C, well above the pyrolysis temperature of most polymers. To resolve this issue, patterned thin films of Cr that have been etched with the commercial etchant Cr-7 (Cyantek Corporation, Fremont, CA) are used to define the channels for μCM to pattern PZT.

3. Surface Modification Techniques

The surface modification methods described here require the deposition of a uniform thin film of the material to be patterned across the substrate. These techniques are subtractive because material is removed from the regions where it is not desired in the final pattern. This is analogous to the first step in patterning in traditional semiconductor fabrication, whereby the photosensitive polymer film is spin-cast from a liquid suspension. Similarly, the thin film of ceramic precursors can be deposited by spin-coating or dip-coating from a solution, such as suspension of solid particles or a sol-gel, followed by a heat treatment for densification and crystallization.

The success of photolithography is due to the photosensitive nature of the polymer films used which permits the definition of patterns due to the selective exposure to light. Using the same principles, some researchers [54–60] have chemically added this functionality to certain sol-gels and chemical solution precursors. However, this technique is not accessible to all chemistries and does not have much value to ceramic thin films derived from colloidal suspensions. A more general surface modification approach called MicroContact Printing (μCP) using self-assembled monolayers [67, 68] can be used instead. The section concludes with a letterpress printing technique that relies on surface tension to confine the liquid to the protruding tips of an inked stamp for pattern transfer.

3.1. Selective Exposure Techniques

The following paragraphs highlight some of the methods by which a deposited thin film can be patterned. Selective exposure methods use an external energy source to convert selected regions of a deposited thin film to non-soluble forms prior to leaching. These processes are analogous to the patterned deposition of an organic thin film positive photoresist layer in semiconductor manufacturing [1]. First, the photosensitive polymer is spin-cast onto the wafer. Next, the film is exposed to ultraviolet (UV) light through a mask. In a positive photoresist, the regions in the film that are exposed to the ultraviolet radiation are cross-linked and rendered insoluble when the wafer is submerged in a developer solution. In the same manner, UV radiation is used to chemically convert regions of the deposited inorganic precursor thin film to a cross-linked form that is insoluble to a leaching solution that removes the undesired regions. The difference between traditional photolithography and selective exposure is that instead of using the patterned photoresist as a mask to transfer the image to another layer of material by wet chemical etch or lift-off techniques, the pattern is directly defined in the inorganic material of interest.

After exposure of the film to UV light, the unexposed regions are removed by dipping the sample in a solvent bath. The patterned ceramic thin film is then converted to its final desired crystalline form by heat treatment. Similar to the other methods described in this paper, shrinkage due to the evaporation of residual solvent or organic compounds, as well due to densification, occurs, resulting in changes to the lateral and vertical dimensions of the patterns.

Preliminary work relied on the effect of using the UV light to accelerate particular sol-gel reactions and reducing the carbon content of the films [54]. Shinmou et al. [55] aimed to broaden the technique by introducing acetylacetone into the gelled films containing Zr-n-butoxides. When exposed to UV light with a wavelength of 300 nm, the $p - p^*$ transition in the chelate ring of the acetylacetone dissociates the chelate bonds in the gel films, reducing the solubility of the films to acidic leaching solutions. After heat treatment, crystalline zirconium oxide (ZrO_2) films with feature sizes of 200 μm were produced. Similarly, Yogo et al. [56] patterned films by adding 1-phenyl-1,3-butanedione, a photosensitive chemical designed to absorb ultraviolet (UV) light at 330 nm, to their precursor solution to pattern lithium niobate ($LiNbO_3$)

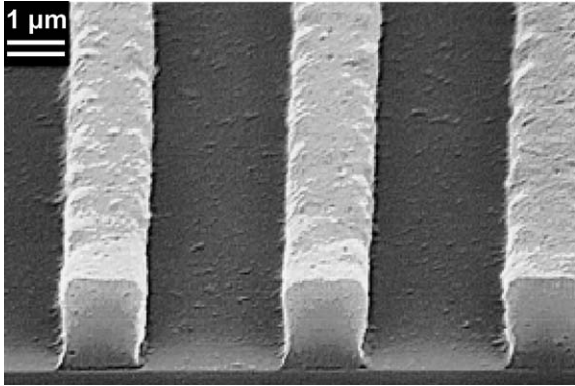

Fig. 7. 1.5 μm SiO_2 lines patterned by photoexposure by Marzolin et al. [59].

films on sapphire substrates. Kikuta et al. patterned titania [57] and tin oxide [58] thin films from precursor solutions doped with UV-sensitive diethanolamine or N-phenyldiethanolamine followed by an ethanol wash. The Whitesides group [59] synthesized a glass photoresist and used photolithography to pattern 1.5 μm wide lines, as shown in Fig. 7. As in photolithography, the feature sizes than can be achieved are limited by the resolution of the mask, equipment optics, and the wavelength of the light source. Using a focused laser beam operating in the UV range, Nakao et al. [60] patterned feature sizes of 0.5 μm.

The primary advantage of this method is that previous experience with photolithography can be used to transfer the desired patterns. Many of the equipment required, such as the UV photomasks, are readily available. Careful control of the irradiation intensity and exposure time are required to achieve the desired resolution; for instance, overexposure can result in roughening of the edge of the patterned lines [56]. A severe disadvantage of the process is that the vertical thickness of the film is limited by the nature of the spin-coating process. It is unclear whether thicker films can be patterned due the need for the sufficient penetration of the energy beam. The thickest materials patterned to date are about 0.4 microns thick [56].

The primary drawback of this technique is that most materials require the alteration of the chemical precursor solution recipe for the addition of compounds sensitive to the wavelength of the UV beam to effect the desired reaction. This greatly limits the choices of materials that can be patterned by this technique. Further, this technique is only applicable to sol-gel based chemistries and can not be used to pattern films derived from colloidal suspensions unless the particles are suspended in a photocurable medium.

A greater selection of materials can be patterned by changing the choice of external energy source to lasers [60–62], ion beams [63], or electron beams [64–66]. These methods selectively pyrolyze the desired regions in the surface using the external energy supplied by the photons, ions, or electrons, eliminating the need to alter the chemistry of the precursor solution. However, these options are beyond the scope of this paper because they require substantial capital investment and are not capable of patterning large areas. These techniques rely upon the serial scanning of the beam across the thin film; while this feature may be desirable due to the ability to custom-write patterns into the thin film oxide, the rate of throughput in an actual production process would be prohibitively slow compared to mask-based processes.

3.2. MicroContact Printing

While elective exposure techniques are based upon transferring a pattern into a previously deposited uniform thin film, μCP [67, 68] relies on the modification of the substrate surface prior to the deposition of the film to effect the final pattern. In the μCP process shown in Fig. 1(d) [9], the PDMS stamp is used to transfer a self-assembled monolayer (SAM) pattern to the substrate. Self-assembly relies on the use of weak interactions to spontaneously organize molecules into a thermodynamically stable structure. SAMs are prepared from ligand molecules of the form $Y(CH_2)_nX$. The anchoring group, Y, is designed to bind to the surface of the substrate, while the head group, X, is tailored to control the surface properties of the monolayer, such as the degree of hydrophilicity. The number of methylene units in the alkyl backbone is used to control the thickness of the SAM. The fidelity of μCP relies on the ability of the molecules to quickly order into a SAM with an autophobicity that prevents the spreading of the monolayer across the surface to non-deposited regions [10].

The patterned SAM layer is then used as a template for the selective deposition of the metal oxide thin film. A chemical precursor solution is spin-coated on top of the substrate with a patterned SAM with hydrophobic end groups, followed by a heat treatment of approximately 300–400°C to pyrolyze the organic components

and to densify the thin film. The regions of the film deposited on top of the SAM show poor adhesion to the substrate surface and crack while the material deposited on the unmodified substrate surface remains firmly bonded. The crazed material is "lifted-off" by mild mechanical abrasion using a cotton felt dampened with isopropanol [9, 69]. Optical microscope images of the film prior to and after this polishing step are shown in Fig. 8 [9, 72]. A higher temperature heat treatment is then used to convert the remaining precursor to the desired crystal structure [9, 69]. The delamination process determines the fidelity of the transferred pattern and appears to be governed by the roughness of the grain boundaries of the underlying substrate [70]. Most researchers chose to deposit the thin film via spin-casting, though selective dip-coating could also be used on surfaces that have been micropatterned into regions of different hydrophilicity [71].

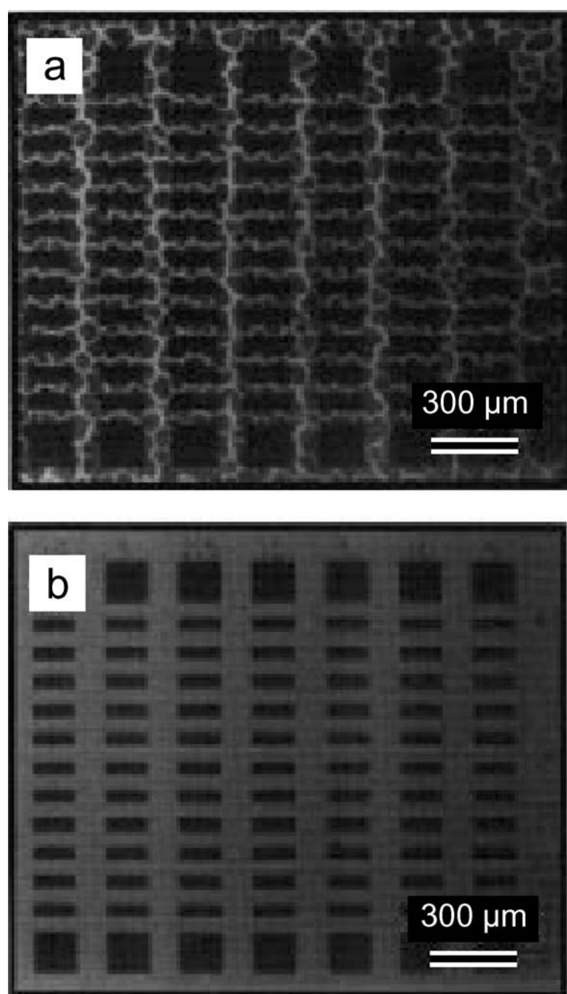

Fig. 8. Optical micrographs of a patterned tantalum oxide film (a) before and (b) after the polishing step [9, 72].

Jeon et al. [69] first reported the use of μCP to pattern a SAM from octadecyltrichlorosilane ($CH_3(CH_2)_{17}SiCl_3$, OTS) in hexanol as a template for depositing lithium niobate ($LiNbO_3$) and lead lanthanum titanate ($Pb_{1-3x/2}La_xTiO_3$) on sapphire, silicon, and indium tin oxide (ITO) substrates. Later work by the same research groups at the University of Illinois at Urbana-Champaign demonstrated the use of the technique for patterning tantalum oxide (Ta_2O_5) on silicon, aluminized silicon, and platinized silicon wafers [70]. They also fabricated ferroelectric memory cells by patterning 200 μm diameter PZT posts on platinized silicon and then using μCP again to pattern platinum on top of the posts [72]. They achieved line widths as small as 4 μm with 100 nm resolution and vertical thickness of 80 to 120 nm with their resulting patterned thin film oxides [70]. Their work is well summarized in a review article [9].

Hwang et al. [73] used chemical bath deposition of CdS particles on Si substrated prepared with OTS patterns by μCP. After ultrasonic agitation to lift off the particles deposited on top of the OTS regions, patterns with boundary resolutions of 100 nm were fabricated. Shin et al. [74] used μCP to pattern an arrangement of hydrophobic SAMs and coated the remainder of the surface with hydrophilic SAMs prior to deposition of iron oxide thin films. Bartz et al. [75] patterned alkane thiols on a gold surface and then coated the unpatterned regions with a thiol terminated with a styrene monomer. The monomer was polymerized prior to the precipitation of a titania film on the surface. A solution of chloroform and trimethylsilyl chloride was used to the polystyrene, leaving behind the patterned titania thin film on top of the alkane SAM. Yan et al. [76] used a variation called Hot MicroContact Printing (HμCP) to transfer a hydrophobic long-chain alkyltrichlorosilane to a less-reactive silicon surface that is heated on a hot plate. Atomic layer epitaxy is used to grow ZnO films on the Si regions not covered by the SAM to produce feature sizes as small as 1 μm. Similarly, Bechiniger et al. [77] used the contrast between hydrophobic and hydrophilic regions to pattern an array of 150 nm tungsten oxide dots from an alkoxide precursor solution. Their PDMS stamp was cast from a self-assembled, hexagonally-arranged, close-packed monolayer of 600 nm diameter polystyrene colloidal spheres.

Another variation of μCP is to print a pattern of acid on top of a continuous thin film to effect the pattern. The Whitesides group [59] inked their elastomeric stamp with hexadecanesulfonic acid in *t*-butyl methyl ether and 2-propanol and printed a pattern on top of a spin-cast glass photoresist. After baking the sample at 130°C for 20 min, the glass was developed in anisole for 20 s. The regions exposed to the acid were cross-linked and rendered insoluble to the developer. This technique was used to pattern lines with edge irregularities of 100 nm.

A number of researchers have produced patterned pattern ceramic thin films, such as TiO_2 [78, 79], ZnO [80, 81], SnO_2 [82], and SiO_2 [83] on top of SAMs that were patterned using exposure to UV light through a mask. Typically, the hydrophobic functional group at the end of the chain is replaced by a hydrophilic hydroxyl. The ceramic material deposited from aqueous solutions preferentially adheres to the hydrophilic regions. Pyrolysis of the SAM during heat treatment steps does not lead to cracking or delamination of the ceramic thin film on the substrate [84]. However, the pyrolysis may leave behind impurities embedded into the oxide layer of the substrate that may impact the performance of the hierarchical device. This issue is not completely mitigated by using μCP to define a pattern of SAMs either, because molecules such as OTS may leave behind graphite contamination after the heat treatment steps and render these regions of the surface unavailable for depositing other materials. The only hierarchical structures that have been fabricated from thin films patterned by μCP are devices whose layers are vertically stacked, such as the isolated ferroelectric capacitors by Jeon et al. [72].

3.3. Letterpress Printing

Letterpress printing is a related technique to μCP whereby the final material to be deposited serves as the "ink" and is directly printed by the mold or "printing plate". The process was first demonstrated with an ink of palladium colloids suspended in toluene printed by PDMS stamps by the Whitesides group [85]. Wang and colleagues [86] patterned dots of polymers using PDMS stamps. Due to their reliance on the presence of solvent to aid the transfer of the polymer from the stamp surface to the substrate, they referred to their process as Micro-Fluid-Contact Printing (μFCP). Miller et al. [87] patterned more complex patterns using both rigid and flexible stamps by maintaining the temperature of the ink and target substrate above the glass transition temperature of the polymer.

As this technique is relatively new, only one demonstration of the technique to ceramic systems has thus been published. Wang et al. [88] applied the same μFCP technique to a composite ink dispersion of TiO_2 colloids dispersed in a hydrolyzed poly(styrene-*alt*-maleic anhydride) copolymer (HSMA). Two-dimensional arrays of 6.8 μm diameter dots were patterned. Currently, the technique is limited to producing discrete circular "dishes" whose thickness at the rims is an order of magnitude greater than at the interior. The dynamics of dewetting of the ink from the stamp to the substrate and the evaporation of the carrier solvent need to be better controlled for this to become a viable technique for ceramic materials.

4. General Limitations

4.1. Materials Limitations

With the exception of letterpress printing, each of the methods presented in this paper has been successfully demonstrated with chemical solution precursors such as sol-gel. Theoretically, letterpress printing could be used with a sol-gel, but it would require solving a number of engineering challenges. Specifically, precise control of the rheological properties to effect the desired pattern transfer from the stamp to the surface is needed. The soft lithography method of μTM suggests that elastomer stamps can be good carriers for sol-gel because the low interfacial energy allows the release of the material when contacted to a substrate with a more beneficial binding energy. For the technique to be a viable alternative, further study on the pressing conditions with both sol-gels and colloidal suspensions is required to eliminate the major topographical distortions that the technique produces [88].

Each of the techniques can also be applied to powder-based chemistries, such as colloidal suspensions. Patterning of thin films derived from ceramic slurries by selective exposure has not yet been reported. To use selective exposure, the colloidal particles would need to be suspended in a photosensitive solvent such as photocurable monomer whose adhesion properties are affected by the application of UV light. The particles themselves can not be directly patterned as they are already comprised of crystalline solid particles whose

adhesion properties will not change in response to the external energy source.

4.2. Resolution Limits

Most of the confinement-based techniques are capable of resolutions on the submicrometer length scale. With the possible exception of MIMIC, there is no reason why these fidelities can not be further improved with the use of finer molds. MIMIC is inherently limited by the requirement of filling the network of capillary channels with relatively viscous chemical solution precursors to produce the pattern. The casting techniques discussed in this paper have not yet been pushed to their resolution limits. Since μCM relies on the same capillary filling principles as MIMIC, there is no reason why it can not be used to define patterns with the same 400 nm feature sizes. Because the work on letterpress printing is relatively new and unproven with ceramic materials, it is not clear what the defining resolution limit of this method. Because of the technique's similarly to μTM in terms of using differences in interfacial energy between the stamp and substrate, letterpress printing should be able to pattern features smaller than one micron once better control of the solution chemistry and printing conditions is established.

4.3. Cracking

The subtractive patterning techniques of selective exposure and μCP have one key limiting feature that may prohibit their use in many applications. Because both techniques rely on spin-casting continuous thin films before production of the final pattern, the films are limited in their thickness. By the Griffith criterion, thin films will crack if they exceed a critical thickness t_c

$$t \geq t_c = \frac{4\omega \cdot E}{Z(1-\nu)\sigma^2} \tag{1}$$

where ω, E, and υ are the specific surface energy, elastic modulus, and Poisson's ratio of the thin film material, Z is a dimensionless geometrical factor, and σ is a constant biaxial stress applied to the film [12, 89]. For many sol-gels, this critical thickness is on the order of 0.1 μm. The fabrication of thicker films requires the repeated spin-casting and heat treatment of multiple layers; the requirement of heat treatment of densify each thin film layer may prohibit the application of the subtractive patterning methods to thicker films.

The issue of cracking is not mitigated by the use of confinement-based techniques. Most of the techniques require a post-patterning heat treatment to densify the thin film and convert the material to the desired crystalline phase. The issue of shrinkage and cracking is still present, but the patterned material is able to release stress in both a lateral direction and the vertical direction. These methods allow the patterning films thicker than permitted in large area continuous thin films as long as the lateral dimension is sufficiently small for the release of sufficient strain energy. For example, Beh et al. [35] reported patterning ZrO_2 lines as wide as 14 μm from molds with 2 μm high channels without cracking, while we have patterned crack-free PZT lines over 20 μm wide from 1.85 μm high channels using MIMIC [34].

5. Conclusion

A summary of the techniques reviewed in this paper is presented in Table 1 with a list of the smallest reported resolution achieved to date. Ultimately, the success of each of the techniques described in this paper will be

Table 1. Summary of patterning techniques for ceramic thin films.

Technique	Sol-Gel	Colloidal dispersions	Resolution
μTM	[17, 25, 26]	[27–29]	500 nm [26]
MIMIC	[24, 33–37, 39–40]	[42]	400 nm [35]
Embossing	[39, 43, 46, 48, 49]	[27, 43, 50–52]	120 nm [43]
Casting	[20]	[53]	5 μm [53]
Selective exposure	[55–60]	Not yet demonstrated	1.5 μm [59]
μCP	[9, 59, 69, 70, 72, 74–77]	[73]	4 μm [70]
Letterpress printing	Not yet demonstrated	[88]	6.8 μm [88]

measured by whether or not it is incorporated into the fabrication scheme for a working device. To date, these techniques have been used for very few applications. Perhaps the most note-worthy example of the incorporation of one of these methods in microfabrication is the use of MIMIC to pattern tin oxide in a gas sensor by Heule and Gauckler [42]. The gas sensor was demonstrated to be able to detect hydrogen and carbon monoxide for concentrations on the order of 100 ppm. The electrode and insulating layers for the device were patterned by traditional photolithography, an indication of how much more convenient and reproducible pattern registry is than by soft lithography. This issue may very well prove to be the Achilles' heel for many of these submicrometer patterning methods as researchers attempt to incorporate them into hierarchical fabrication schemes.

Acknowledgments

The main portion of the authors' work is supported by NASA grant NAG-2-1475. Partial support by the NASA University Research, Engineering, and Technology Institute on BioInspired Materials (BIMat) under award NCC-1-02037 is also acknowledged.

References

1. S.A. Campbell, *The Science and Engineering of Microelectronic Fabrication* (Oxford University Press, New York, 1996).
2. T. Ito and S. Okazaki, *Nature*, **406**, 1027 (2000).
3. C. Hageleitner, A. Hierlemann, D. Lange, A. Kummer, N. Kerness, O. Brand, and H. Baltes, *Nature*, **414**, 293 (2001).
4. D.L. Polla and L.F. Francis, *Annu. Rev. Mater. Sci.*, **28**, 563 (1998).
5. S. Ono and S. Hirano, *J. Am. Ceram. Soc.*, **80**, 2533 (1997).
6. N. Ozawa and T. Yao, *Solid State Ionics*, **151**, 79 (2002).
7. K. Nashimoto, K. Haga, M. Watanabe, S. Nakamura, and E. Osakabe, *Appl. Phys. Lett.*, **75**, 1054 (1999).
8. J.F. Scott and C.A. Paz de Araujo, *Science*, **246**, 1400 (1989).
9. D.A. Payne and P.G. Clem, *J. Electroceram.*, **3**, 163 (1999).
10. Y. Xia and G.M. Whitesides, *Annu. Rev. Mater. Sci.*, **28**, 153 (1998).
11. A. Roelofs, T. Schneller, K. Szot, and R. Waser, *Appl. Phys. Lett.*, **81**, 5231 (2002).
12. F.F. Lange, *Science*, **273**, 903 (1996).
13. R.W. Schwartz, *Chem. Mater.*, **9**, 2325 (1997).
14. P.F. Blazdell, J.R.G. Evans, M.J. Edirisinghe, P. Shaw, and M.J. Binstead, *J. Mater. Sci. Lett.*, **14**, 1562 (1995).
15. M. Mott, J.-H. Song, and J.R.G. Evans, *J. Am. Ceram. Soc.*, **82**, 1653 (1999).
16. P. Calvert, *Chem. Mater.*, **13**, 3299 (2001).
17. X.-M. Zhao, Y. Xia, and G.M. Whitesides, *J. Mater. Chem.*, **7**, 1069 (1997).
18. T.W. Odom, J.C. Love, D.B. Wolfe, K.E. Paul, and G.M. Whitesides, *Langmuir*, **18**, 5314 (2002).
19. A. Folch and M.A. Schmidt, *J. Microelectromech. S.*, **8**, 85 (1999).
20. C.R. Martin and I.A. Aksay, submitted.
21. X.M. Zhao, Y.N. Xia, and G.M. Whitesides, *Adv. Mater.*, **8**, 837 (1996).
22. E. Kim, Y. Xia, and G.M. Whitesides, *Nature*, **376**, 581 (1995).
23. Y. Xia, E. Kim, and G.M. Whitesides, *Chem. Mater.*, **8**, 1558 (1996).
24. E. Kim, Y. Xia, and G.M. Whitesides, *J. Am. Chem. Soc.*, **118**, 5722 (1996).
25. J.H. Kim, F.F. Lange, and C.-I. Choen, *J. Mater. Res.*, **14**, 1194 (1999).
26. P.M. Moran and F.F. Lange, *Appl. Phys. Lett.*, **74**, 1332 (1999).
27. U.P. Schönholzer, N. Stutzmann, T.A. Tervoort, P. Smith, and L.J. Gauckler, *J. Am. Ceram. Soc.*, **85**, 1885 (2002).
28. U.P. Schönholzer and L.J. Gauckler, *Adv. Mater.*, **11**, 630 (1999).
29. B. Su, D. Zhang, and T.W. Button, *J. Mater. Sci.*, **37**, 3123 (2002).
30. E. Kim and G.M. Whitesides, *J. Phys. Chem. B*, **101**, 855 (1997).
31. N.L. Jeon, I.S. Choi, B. Xu, and G.M. Whitesides, *Adv. Mater.*, **11**, 946 (1999).
32. G. Yi, Z. Wu, and M. Sayer, *J. Appl. Phys.*, **64**, 2717 (1988).
33. J.S. Vartuli, M. Özenba, C.-M. Chun, M. Trau, and I.A. Aksay, *J. Mater. Res.*, **18**, 1259 (2003).
34. C.R. Martin and I.A. Aksay, *J. Phys. Chem. B.*, **107**, 4261 (2003).
35. W.S. Beh, Y. Xia, and D. Qin, *J. Mater. Res.*, **14**, 3995 (1999).
36. S. Seraji, Y. Wu, N.E. Jewell-Larson, M.J. Forbess, S.J. Limmer, T.P. Chou, and G. Cao, *Adv. Mater.*, **12**, 1421 (2000).
37. M. Trau, N. Yao, E. Kim, Y. Xia, G.M. Whitesides, and I.A. Aksay, *Nature*, **390**, 674 (1997).
38. A.Y. Ku, doctoral dissertation, Princeton University, 2003.
39. P. Yang, T. Deng, D. Zhao, P. Feng, D. Pine, B.F. Chmelka, G.M. Whitesides, and G.D. Stucky, *Science*, **282**, 2244 (1998).
40. M. Yu, J. Lin, Z. Wang, J. Fu, S. Wang, H.J. Zhang, and Y.C. Han, *Chem. Mater.*, **14**, 2224 (2002).
41. X.M. Han, J. Lin, R.B. Xing, J. Fu, and S.B. Wang, *Mater. Lett.*, **57**, 1355 (2003).
42. M. Heule and L.J. Gauckler, *Adv. Mater.*, **13**, 1790 (2001).
43. C.A. Bulthaup, E.J. Wilhelm, B.N. Hubert, B.A. Ridley, and J.M. Jacobson, *Appl. Phys. Lett.*, **79**, 1525 (2001).
44. S.Y. Chou, P.R. Krauss, and P.J. Renstrom, *Science*, **272**, 85 (1996).
45. S.Y. Chou, P.R. Krauss, W. Zhang, L. Guo, and L. Zhuang, *J. Vac. Sci. Technol. B*, **15**, 2897 (1997).
46. C. Marzolin, S.P. Smith, M. Prentiss, and G.M. Whitesides, *Adv. Mater.*, **10**, 571 (1998).
47. E. Delamarche, H. Schmid, H.A. Biebuyck, and B. Michel, *Adv. Mater.*, **9**, 741 (1997).
48. O.J.A. Schueller, G.M. Whitesides, J.A. Rogers, M. Meier, and A. Dodabalapur, *Appl. Optics*, **38**, 5799 (1999).
49. A. Matsuda, Y. Matsuno, M. Tatsumisago, and T. Minami, *J. Am. Ceram. Soc.*, **81**, 2849 (1998).
50. S. Petronis, K.-L. Eckert, J. Gold, and E. Wintermantel, *J. Mater. Sci.-Mater. Med.*, **12**, 523 (2001).

51. B. Su, T.W. Button, A. Schneider, L. Singleton, and P. Prewett, *Microsyst. Technol.*, **8**, 359 (2002).
52. A. Schneider, B. Su, T.W. Button, L. Singleton, O. Wilhelmi, S.E. Huq, P.D. Prewett, and R.A. Lawes, *Microsyst. Technol.*, **8**, 88 (2002).
53. U.P. Schönholzer, R. Hummel, and L.J. Gauckler, *Adv. Mater.*, **12**, 1261 (2000) .
54. T. Ohishi, S. Maekawa, and A. Katoh, *J. Non-Cryst. Solids*, **147/148**, 493 (1992).
55. K. Shinmou, N. Tohge, and T. Minami, *Jpn. J. Appl. Phys.*, **33**, L1181 (1994).
56. T. Yogo, Y. Takeichi, K. Kikuta, and S.-I. Hirano, *J. Am. Ceram. Soc.*, **78**, 1649 (1995).
57. K. Kikuta, K. Takagi, and S. Hirano, *J. Am. Ceram. Soc.*, **82**, 1569 (1999).
58. K. Kikuta, K. Suzumori, K. Takagi, and S. Hirano, *J. Am. Ceram. Soc.*, **82**, 2263 (1999).
59. C. Marzolin, A. Terfort, J. Tien, and G.M. Whitesides, *Thin Solid Films*, **315**, 9 (1998).
60. Y. Nakao, T. Nakamura, K. Hoshiba, K. Sameshima, A. Kamisawa, K. Abe, N. Soyama, and K. Ogi, *Jpn. J. Appl. Phys.*, **32**, 4141 (1993).
61. J.V. Mantese, A.B. Catalan, A.M. Mance, A.H. Hamdi, A.L. Micheli, J.A. Sell, and M.S. Meyer, *Appl. Phys. Lett.*, **53**, 1335 (1988).
62. T. Toshiyuki, N. Ichinose, S. Kawanishi, M. Nishii, T. Sasuga, I. Hashida, and K. Mizuno, *Chem. Mater.*, **9**, 2674 (1997).
63. L.S. Hung and L.R. Zheng, *Appl. Phys. Lett.*, **60**, 2210 (1992).
64. S. Okamura, Y. Yagi, S. Ando, T. Tsukamoto, and K. Mori, *Jpn. J. Appl. Phys.*, **33**, 6579 (1996).
65. A. Kakimi, S.Okamura, Y. Yagi, K. Mori, and T. Tsukamoto, *Jpn. J. Appl. Phys.*, **33**, 5301 (1994).
66. K. Mori and S. Okamura, *Jpn. J. Appl. Phys.*, **31**, L1143 (1992).
67. A. Kumar and G.M. Whitesides, *Appl. Phys. Lett.*, **63**, 2002 (1993).
68. A. Kumar, H.A. Biebuyck, and G.M. Whitesides, *Langmuir*, **10**, 1498 (1994).
69. N.L. Jeon, P.G. Clem, R.G. Nuzzo, and D.A. Payne, *J. Mater. Res.*, **10**, 2996 (1995).
70. P.G. Clem, N.-L. Jeon, R.G. Nuzzo, and D.A. Payne, *J. Am. Ceram. Soc.*, **80**, 2821 (1997).
71. A.A. Darhuber, S.M. Troian, J.M. Davis, S.M. Miller, and S. Wagner, *J. Appl. Phys.*, **88**, 5119 (2000).
72. N.L. Jeon, P. Clem, D.Y. Jung, W. Lin, G.S. Girolami, D.A. Payne, and R.G. Nuzzo, *Adv. Mater.*, **9**, 891 (1997).
73. Y.K. Hwang, S.Y. Woo, J.H. Lee, D.-Y. Jung, and Y.-U. Kwon, *Chem. Mater.*, **12**, 2059 (2000).
74. H. Shin, J.U. Jeon, Y.E. Pak, H. Im, and E.S. Kim, *J. Mater. Res.*, **16**, 564 (2001).
75. M. Bartz, A. Terfort, W. Knoll, and W. Tremel, *Chem. Eur. J.*, **6**, 4149 (2000).
76. M. Yan, Y. Koide, J.R. Babcock, P.R. Markworth, J.A. Belot, T.J. Marks, and R.P.H. Chang, *Appl. Phys. Lett.*, **79**, 1709 (2001).
77. C. Bechinger, H. Muffler, C. Schäfle, O. Sundberg, and P. Leiderer, *Thin Solid Films*, **366**, 135 (2000).
78. R.J. Collins, H. Shin, M.R. DeGuire, A.H. Heuer, and C.N. Sukenik, *Appl. Phys. Lett.*, **69**, 860 (1996).
79. K. Koumoto, S. Seo, T. Sugiyama, W.S. Seo, and W.J. Dressick, *Chem. Mater.*, **11**, 2305 (1999).
80. N. Saito, H. Haneda, W.-S. Seo, and K. Koumoto, *Langmuir*, **17**, 1461 (2001).
81. N. Saito, H. Haneda, T. Sekiguchi, N. Ohashi, I. Sakaguchi, and K. Koumoto, *Adv. Mater.*, **14**, 418 (2002).
82. N. Shirahata, Y. Masuda, T. Yonezawa, and K. Koumoto, *Langmuir*, **18**, 10379 (2002).
83. Y. Masuda, W.S. Seo, and K. Koumoto, *Jpn. J. Appl. Phys.*, **39**, 4596 (2000).
84. H. Shin, Y. Wang, U. Sampathkumaran, M.R. DeGuire, A.H. Heuer, and C.N. Sukenik, *J. Mater. Res.*, **14**, 2116 (1999).
85. P.C. Hidber, W. Helbig, E. Kim, and G.M. Whitesides, *Langmuir*, **12**, 1375 (1996).
86. M. Wang, H.-G. Braun, T. Kratzmüller, and E. Meyer, *Adv. Mater.*, **13**, 1312 (2001).
87. S.M. Miller, S.M. Troian, and S. Wagner, *J. Vac. Sci. Technol. B*, **20**, 2320 (2002).
88. M. Wang, H.-G. Braun, and E. Meyer, *Chem. Mater.*, **14**, 4812 (2002).
89. J.W. Hutchinson and Z. Suo, *Adv. Appl. Mech.*, **29**, 63 (1992).